

# Effect of hydrogen addition on MILD combustion in an industrial furnace

**M. Ferrarotti<sup>1,2,3</sup>, S. Vicens de Cabo<sup>1</sup>, A. Fita-Codina<sup>1,3</sup>, W. de Paepe<sup>2</sup>, A. Parente<sup>1,3</sup>**

1. Université Libre de Bruxelles, École polytechnique de Bruxelles, Aero-Thermo-Mechanics Laboratory, 1050 Bruxelles, Belgium
2. Thermal Engineering and Combustion Unit, Université de Mons (UMONS), 7000 Mons, Belgium
3. Combustion and Robust Optimization Group (BURN), Université Libre de Bruxelles and Vrije Universiteit Brussel, 1050 Bruxelles, Belgium

## INTRODUCTION

Energy is undoubtedly the single most important factor impacting the prosperity of our society. Nowadays, renewable intermittent energy sources are integrated with combustion-based energy production system. However, the massive penetration of renewables will lead to electricity excess that could be advantageously stored as a fuel through Power-to-Fuel (P2F), to assure short, medium and especially, long-term storage.

However, this concept needs a fuel and thermal load flexibility, which is not an easy task to pursue in a single combustion unit. Indeed, the latter is normally optimized to work within a well identified range of operational parameters and with a limited possibility for fuel choice. This is needed to achieve a flame stabilization, which is fuel and configuration dependent, to maximize efficiency and reduce pollutant emission. Moreover, this new generation of fuels includes blends of different gases ( $\text{CH}_4$ ,  $\text{H}_2$ ,  $\text{NH}_3$ ,  $\text{CO}$ ,  $\text{CO}_2$ , ...), produced by a wide variety of processes, with the general aim of maximizing the renewability of the sources. As a consequence, the development of load and fuel-flexible, efficient and environmentally friendly combustion technologies appears to be crucial. Among them, flameless or Moderate or Intense Low-oxygen Dilution (MILD) combustion [1,2] has attracted increasing attention. It is characterized by diluted reactants to locally reach mixture autoignition temperature, non-visible flame and uniform distributed temperature [3]. On the other hand, dilution prevents the stabilization of deflagrative/diffusive structures, as a consequence of the local autoignition.

The potential of MILD combustion in terms of energy efficiency and pollutant emissions has been thoroughly investigated by several authors, such as Katsuki and Hasegawa [4], de Joannon et al. [5], Khalil and Gupta [6] and valuable knowledge has been obtained to clarify the fundamental mechanisms governing such a combustion technology. At the same time, in the last few decades, different studies have been conducted in standard model reactors [5, 7] and on laboratory-scales burners, built to emulate MILD combustion. Among them, the Adelaide Jet in Hot Co-flow (AJHC) burner [8] and the Delft Jet in Hot Co-flow (DJHC) [9] have received significant attention from the combustion community, serving as reference data sets for the validation of turbulent combustion models. Recently, efforts have been spent to develop systems that can more faithfully reproduce the conditions met in realistic applications, bridging the gap from laboratory to industrial scale [10, 11, 12].

Despite the reasonable number of studies in the literature listed above, the amount of detailed experimental data available for combustors operating under MILD conditions is relatively scarce and limited to few operating conditions. In this framework, the present paper aims at improving the knowledge of MILD combustion in industrial burner. Experiments have been carried out to prove the feasibility of MILD combustion using methane/hydrogen mixtures and the key role of hydrogen in reducing the ignition delay time.

## EXPERIMENTAL SETUP AND METHODOLOGY

The experimental campaign was conducted on a 20 kW MILD combustion furnace [11]. It consists in a cubic combustion chamber ( $1100 \times 1100 \times 1100 \text{ mm}^3$ ) coupled with a FLOX burner, characterized by an integrated metallic finned heat exchanger to extract energy from the flue gases and to pre-heat the combustion air. The combustion chamber itself is made of stainless steel and has a cubic internal section of 700 mm on each side, having a 200-mm-thick high temperature ceramic fiberboard insulation. Fuel and air are fed co-axially into the combustion chamber, through separated jets. The unit is equipped with an air-cooling system consisting of four cooling tubes (OD 80 mm), with a length of 630 mm inside the furnace. Varying the air flow allows the combustion chamber to operate at different stable conditions, thus simulating the effect of a variable load. On each vertical wall of the combustion chamber, an opening is available for measurements. One side is equipped with a  $110 \times 600 \text{ mm}$  quartz window and other with six measurement ports.

The position and shape of the reaction/heat release zone was identified via OH\* chemiluminescence imaging, using an ICCD (Intensified Charge-coupled device) camera 1.4 M, coupled with a 78 mm UV lens F/3.8 and UV bandpass filter (240–400 nm). The intensifier (IRO) gain was set to 80 with an acquisition frequency of 17 Hz. This allow to investigate a portion of the furnace going from 60 to 660 mm along the vertical axis. The background noise was removed, and an averaged image and the related standard deviation were then extracted. Besides that, the in-flame temperature was also measured, thanks to an air-cooled suction pyrometer equipped with a B-type thermocouple (Pt-Rh 30%/Pt-Rh 6%). Further details can be found in [11]. According to the manufacturer's specifications, the systematic uncertainty associated is the 0.5 % of the reading.

The mixtures were created from pure gases in bottles thanks to a static mixer fed. The mass flow rates were regulated using several mass flow controllers ( $\pm 0.9\%$  of S.P.). Finally, the exhaust gas composition was sampled at the exit section through an HORIBA MEXA-ONE FT FTIR analyzer. Based on the absorption spectra, the concentration of  $\text{NO}_x$  was determined. The linearity error and the zero noise for  $\text{NO}_x$  emissions were both equals to  $\pm 2 \text{ ppm}$ . The emissions were then normalized to 3%  $\text{O}_2$ .

Experimental tests were conducted using methane/hydrogen mixtures, keeping a constant thermal input power (20 kW), equivalence ratio ( $\phi=0.8$ ) and cooling flow rate. Three different mixtures were tested: 100%  $\text{CH}_4$ , 90-10%  $\text{CH}_4/\text{H}_2$  and 70-30%  $\text{CH}_4/\text{H}_2$  in volume basis.

## RESULTS

From the analysis of the in-flame temperature measured at different axial positions and the main OH\* images (see Fig. 1 and 2), it emerges that for pure methane (100%  $\text{CH}_4$ ), the oxidation occurs at the margins (and probably beyond) of the window, close to the top wall, with a homogeneous temperature distribution. Instead, when hydrogen is added to the fuel (Fig. 1 and Fig. 2b and c, cases 90/10% and 70/30%), the ignition zone is shifted more and more backward and the number of OH\* counts drastically increases. In particular, the case 90/10% (vol.) shows relevant similarities with the methane case. Indeed, an increase of temperature of less than 10% can be only observed at  $x=600 \text{ mm}$ . On the contrary, once a relevant quantity of hydrogen is injected in the fuel (30% vol.), a well-defined higher temperature region is observed, always within the MILD combustion condition limits ( $T_{\max}-T_{\min} < T_{\text{auto-ignition}}$ ). The reaction region appears shifted backwards in a region between 300 mm and 420 mm from the burner exit along the vertical direction  $x$ . Hydrogen has a significant impact on the radical pool and, then, it directly affects the ignition process, reducing the ignition delay time, typical of MILD combustion of methane. It is also important to keep in mind that hydrogen is highly diffusive and highly buoyant gas, thus it rapidly mixes with the surrounding helping the reaction to be extended in a wider volume. On the other hand, since the thermal input power was not changed during tests, it means that a relevant in-

crease of fuel flow rate (26%) was introduced into the chamber, enhancing the fuel penetration into the air jet.

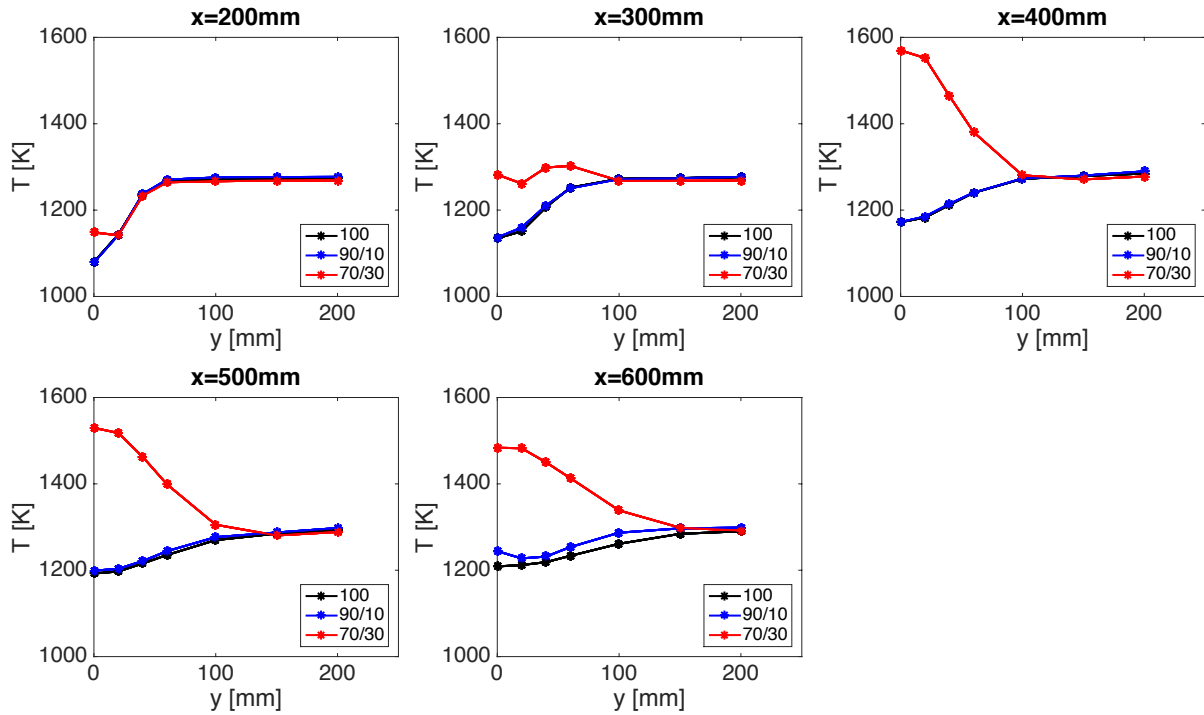


Figure 1. In-flame temperature measurements at different axial positions for the cases: 100%  $\text{CH}_4$ , 90/10%  $\text{CH}_4/\text{H}_2$  and 70/30%  $\text{CH}_4/\text{H}_2$ , highlighting the backwards shift in reaction zone when  $\text{H}_2$  is added to the fuel. Global averaged uncertainty of 5K.

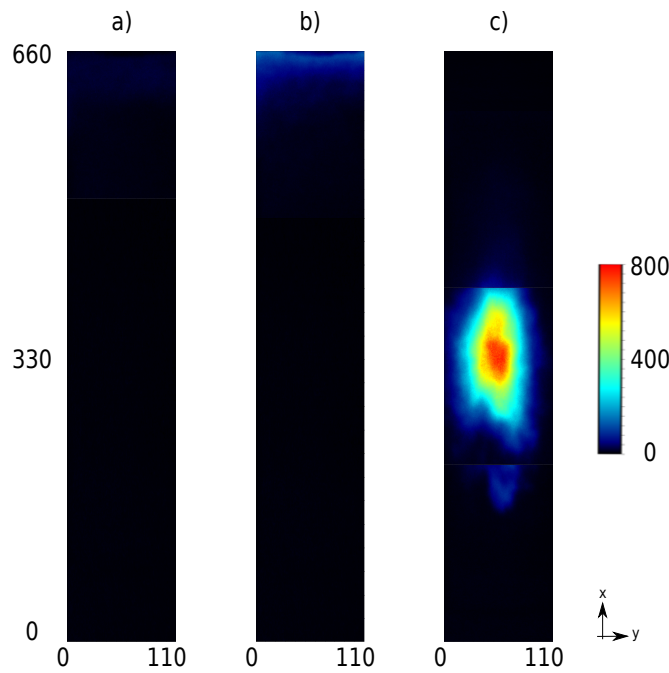


Figure 2. Mean image of  $\text{OH}^*$  counts for a) 100%  $\text{CH}_4$  b) 90/10%  $\text{CH}_4/\text{H}_2$  and c) 70/30%, highlighting the backwards shift in reaction zone when  $\text{H}_2$  is added to the fuel. Units in mm.

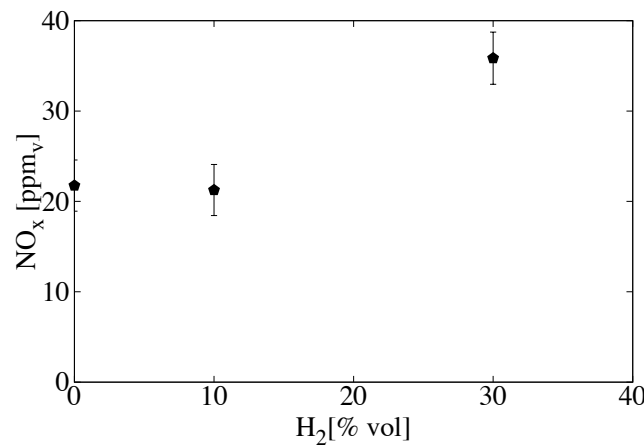


Figure 3. Dry NO<sub>x</sub> emissions normalized at 3% O<sub>2</sub> in function of the H<sub>2</sub> molar fraction in the fuel.

Figure 3 shows the dry NO<sub>x</sub> emissions normalized at 3% O<sub>2</sub> at the outlet section. Considering that, in MILD combustion, the thermal pathway is not the main NO source, other routes become important, such as prompt, N<sub>2</sub>O, and NNH. The latter is relevant in presence of H<sub>2</sub> and it could explain the increasing trend visible in Fig. 3.

## CONCLUSIONS

Experimental tests were performed with the aim of testing the feasibility of achieving MILD combustion and its fuel flexibility. Different methane/hydrogen mixtures were tested keeping the same input power, equivalence ratio and cooling flow rate. Results show the key role of hydrogen in reducing the ignition delay time typical of methane. Indeed, the ignition zone is shifted more backward closer to the burner exit. NO<sub>x</sub> emissions slightly increase injecting more hydrogen, since the NNH pathway becomes more important.

## ACKNOWLEDGEMENTS

This project has received funding from the Fonds de la Recherche Scientifique (FNRS), Belgium. The research of A. Parente was sponsored by the European Research Council, Starting Grant 714605, and from the Fédération Wallonie-Bruxelles, via Les Actions de Recherche Concertée (ARC) call for 2014– 2019.

## REFERENCES

- [1] J. Wüning, J. Wüning, Prog. Energy Combust. Sci. 23 (1) (1997) 81–94.
- [2] A. Cavaliere, M. de Joannon, Prog. Energy Combust. Sci. 30 (4) (2004) 329–366.
- [3] M. de Joannon, G. Sorrentino, A. Cavaliere, Combust. Flame 159 (5) (2012) 1832–1839.
- [4] M. Katsuki, T. Hasegawa, Proc. Combust. Inst. 1998, 27, 3135–3146.
- [5] M. de Joannon, A. Cavaliere, T. Faravelli, E. Ranzi, P. Sabia, A. Tregrossi, Proc. Combust. Inst. 2005, 30, 2605–2612.
- [6] A. E. E. Khalil, A. K. Gupta, Fuel 2016, 182, 17–26.
- [7] T. Le Cong, P. Dagaut, Proc. Combust. Inst. 2009, 32, 427–435.
- [8] B. B. Dally, A. N. Karpets, R. S. Barlow, Proc. Combust. Inst. 2002, 29, 1147–1154.
- [9] E. Oldenhof, M. J. Tummers, E. H. van Veen, D. J. E. Roekaerts, Combust. Flame 2011, 158, 1553–1563.
- [10] P. Sabia, G. Sorrentino, P. Bozza, G. Ceriello, R. Ragucci, M. de Joannon, Proc. Combust. Inst. 2018.
- [11] M. Ferrarotti, M. Fürst, E. Cresci, W. de Paepe, A. Parente, Energy Fuels 2018, 32, 10, 10228–10241.
- [12] A. F. Colorado, B. A. Herrera, A. A. Amell, Bioresour. Technol. 2010, 101, 2443–2449.